Performance Analysis Of A Commercial Agricultural UAV Multispectral Sensor From Imaging Optics To Bands Sensitivity Response From 350nm To 1000nm Range In The Determination Of Selected Vegetation Indices

Bernardino Buenaobra[1,2], Mark Manhuyod[4], Rheo Bernard Gataber[4], Ian Lumiano[5], Michelle Abarca[4], Benjamin Mabanta[4] and Roland Otadoy[1,2]

[1]USC Phil-LiDAR Research Center, University of San Carlos
Nasipit Rd. Talamban, Cebu City Cebu Philippines 6000
Email:bjbuenaobra@usc.edu.ph
[2]Department of Physics, School of Arts and Sciences, University of San Carlos
Nasipit Rd. Talamban, Cebu City, Cebu, Philippines 6000
Email:rolandotadoy2012@gmail.com
[4]Department of Geomatics and Analytics, Del Monte Philippines Inc.
M.Fortich Bukidnon, Philippines 8705
Email: manhuyodjmv@delmonte-phil.com, gataberrp@delmonte-phil.com,
abarcamb@delmonte-phil.com, mabantabz@delmonte-phil.com
[5]Agricultural Research Department,Del Monte Philippines Inc.
M.Fortich,Bukidnon, Philippines 8705
Email:lumianoib@delmonte-phil.com

KEYWORDS: vegetation index, UAV, multispectra, ground sampling distance,sensors

ABSTRACT: The performance of two representative commercial multispectral sensors employed for agricultural UAVs have been analyzed in terms of their imaging and spectral response. We considered primarily a key performance parameter gathered from the response of two independent sensors called Ground Sampling Distance (GSD). Since GSD is the distance between two consecutive pixel centers measured on the ground this could be a differentiating factor for the selection of sensors. One sensor device known as Model m4C (Airinov France) gave a resolution 5.3 cm/pixel@50m in the GR+Red Edge+NIR bands while another sensor in consideration known as Model Red Edge (Micasense US) was specified at 8 cm/pixel@120m flight altitude for BGR+Red Edge+NIR in single camera package. Using known ground truth spectral data signatures obtained by a field spectrometer from plant specimens, we performed a frequency analysis involving overlaying the 4 and 5 discrete bands of these sensors with the test signature. We obtain the peaking under each these discrete bands and used the result for calculation of a select set of vegetation indices. Our interest focused on the sensor response in the bands where the key vegetation index NDVI is calculated and extends these calculations to obtain other indices such as GR, GRVI, RVI, EVI, CIgreen and CIrededge. For purposes of comparison, the same plant spectral signature was overlaid with Landsat 8 OLI visible B2, B3, B4 and the infrared B5 reflectance bands. When the plant spectral signature is taken as true value, the results of comparison in the test case for the NDVI showed a significant difference in the percentage error to Landsat 8 sensors band that could be high as 54% for the 4mC and 50% for the Red Edge sensor however, between the UAV sensors they practically track each other at about 7% to 8% error. Our results show that Red and NIR band sensitivity on how they are designed will determine their effectiveness in the quantification indices that absorb or reflect these wavelengths. Furthermore, the location of the center frequencies and the width of the their spectral response in the image sensors will have to be selected considering advanced knowledge plant or leaf dynamics where its spectral signature would rest.

1 INTRODUCTION

The rise of unmanned aerial vehicles (UAV) technologies (Business Insider: The Drones Report 2015) has enabled rapidly the assessment vegetation vigor and health on large farm areas and agricultural plantation at an airborne height from 50m to 200m well below the clouds. Depending on wind speed and make up of the vegetation areas, a typical fixed wing UAV has a productivity of 100 hectares/flight of land area with a maximum battery usage of around 30-40 minutes. In contrast with imagery from a space orbiting satellite at distances 400km-750km altitude above earths surface, an UAV is considered as airborne photogrammetry class system. While UAV uses Ground Sampling Data (GSD) as its horizontal footprint measured in cm/pixel as the smallest distance it can resolve in an imagery, UAV images can be as 5x better than those offered by Landsat 8 OLI missions (USGS.,2016a) for a more closer detailed localized area of study at the centimeter resolution.

However, the UAV sensors are less superior compared with the satellite bands in terms of frequency response and sensitivity.There are typically 5 bands for a multispectral sensor as compared, for example, for an eleven (11) discrete 30-m bands of Landsat 8 per earth pixel. At the most they can be improved by preprocessing, subsetting a smaller area and performing a two dimensional interpolation with a single dedicated 15-m panchromatic band. One important objective of this paper is to determine the figure of merit from the UAV sensors in its response to the visible (VIS) and the invisible near infrared (NIR) bands especially when measurement of vegetation health and vigor are considered such as NDVI. This paper exhibits our analysis and reports on the key performance parameter from two selected commercial UAV sensors using test data from field work flight missions from a plantation study area. Fundamental optical, image and flight parameters will be discussed in the following subsection to lead the reader to important key points when considering acquiring UAV sensors.

1.1 Ground Sampling Data (GSD) as measure of UAV ground resolution

The primary consideration in the selection of the UAV must be the specification for highest resolution of sensor at the ground when viewed from a certain flight altitude. The Ground Sampling Distance (GSD) is the distance between two consecutive pixel centers measured on the ground. Given the nearness or closeness between these two pixels at ground, the ability to discriminate them is the ultimate measure of its resolving power. Numerically interpreted, the bigger the value of the image GSD, the lower the spatial resolution of the image hence, the less visible details. The GSD is also related to the flight height, the higher the altitude of the flight, the larger the GSD value.

1.1.1 Parameters in a GSD ray trace geometry

To relate the highest resolution at ground of the GSD as seen by the UAV sensor, The geometrical parameters involve the image sensor size, the focal length of the lens as it relates to horizontal field of view (FOV) and the working distance from the last surface of the lens to the object. Figure 1 below depicts the geometry for the GSD. here we define $s = \Delta AB$ as the image sensor size while $d = \Delta CC'$ as the last surface of the camera

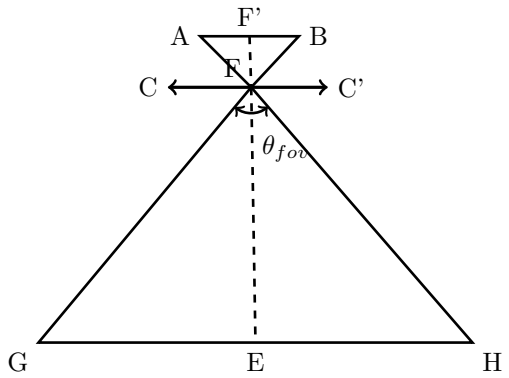

Figure 1: The GSD geometry forms a similar triangle that shows the relationship among these parameters as to sensor size, focal length of the lens, field of view with flight altitude to obtain the resolution at ground. (not drawn to scale)

lens system with a specification for focal length $fl = \Delta FF'$, the field of view at point F as $fov = \Delta GH$ and the working distance $wd = \Delta FE$ as the maximum flight altitude of the UAV. Two equal angles $\theta/2$ are formed comprising of $\angle EH$ and $\angle EG$ which are equal and are defined here as half angle view given by:

$$\frac{\theta_{fov}}{2} = \arctan\left(\frac{\Delta EH}{\Delta FH}\right) = \arctan\left(\frac{\Delta EG}{\Delta FG}\right) \tag{1}$$

the complete field of view angle therefore when referenced to the line that divides the lower triangle ΔGFH from F to E to its left and to its right will be the sum of two half angles view as follows:

$$\theta_{fov} = \theta_{\angle EH} + \theta_{\angle EG} \tag{2}$$

By symmetry the imaging will require $\theta_{\angle EH} = \theta_{\angle EG}$ hence, one half angle view is the same as having each angle doubled to satisfy the full angle field of views.

$$\theta_{fov} = 2\theta_{\angle EH} = 2\theta_{\angle EG} \tag{3}$$

At ground our interest is what can be covered by the UAV, for a half angle view at a certain assigned flight altitude we would be able to obtain the following:

$$\Delta EH = \Delta FH \tan\left(\frac{\theta_{fov}}{2}\right) = \Delta FH \tan\theta_{\angle EH} \tag{4}$$

$$\Delta EG = \Delta FG \tan\left(\frac{\theta_{fov}}{2}\right) = \Delta FG \tan\theta_{\angle EG} \tag{5}$$

The entire coverage of the UAV along its horizontal path of flight in terms of the distances will consequently change with the change in the sum of each half angle field of views that is:

$$\Delta FOV = \Delta EH + \Delta EG \tag{6}$$

While the working distance wd between the ground and the last surface that is ΔFE from the camera sensor lens can be derived by Pythagorean Theorem that would yield the same results because of the symmetry for the distances are given:

$$\Delta FE = \sqrt{\Delta FH^2 - \Delta EH^2} = \sqrt{\Delta FG^2 - \Delta EG^2} \tag{7}$$

For commercial UAV, flight altitudes can be as low as 50m and can be as high as 150m to 200m with pixel resolution on their data sheets for the multispectral sensor as high as 5.3cm/pixel at assigned altitude of 50m. A spreadsheet calculator is available from Micasens website (Micasense Red Edge Data Sheet.,2016) to allow the calculation of the resolution that can be attained relating the optical and machine vision parameters.

1.1.2 Sensor optics and imaging parameters for the UAV

We show in this section the development of relationship between the optical and vision parameters with those flight operating variables from the UAV such as flight altitude and horizontal field of view. This led us to arrive at a functional relationship for understanding the practical performance of real world UAVs. Referring back to Figure 1, we used the Angle Construction Theorem to show that there exist similar triangles in the Ground Sampling Data (GSD) geometry. To check for the similarity, consider the triangle $\triangle HGB$ a ray trace $\overrightarrow{GB}$ that is such that $\angle HGF \cong \angle A$. Similarly, there exist a ray trace $\overrightarrow{HA}$ such that $\angle GHA \cong \angle B$. Moreover, if the sum of the measures of $\angle A$ and $\angle B$ is also less than 180° it follows that the measures of $\angle HGF$ and $\angle GHA$ also sum to less than 180°. Applying the Euclid′s Postulate, we can find a point F on that same side of $\overleftrightarrow{GH}$ where the lines $\overleftrightarrow{GB}$ and $\overleftrightarrow{HA}$ intersect. By the AA Similarity Theorem we see that $\triangle HGF \sim \triangle ABF$. From this deduction we apply the Fundamental Theorem of Similar Triangles then:

$$\frac{HG}{AB} = \frac{HF}{AF} = \frac{GF}{BF} \tag{8}$$

Note that $s = \Delta AB$ is for the image sensor size, field of view is $fov = \Delta HG$, while $\Delta AF = \Delta BF$ are distances where for focal length fl of the lens can be derived and $\Delta HF = \Delta GF$ where the flight altitude FE can be obtained by similar triangles considering that these vertices are scaled versions of each other and their angles are congruent. Rewriting Equation (8) in terms of the optical and flight parameters, the resulting equation would be:

$$\frac{fov}{s} = \frac{wd}{fl} \tag{9}$$

This result shows that all four parameters for optics and flight are contained in one equation which is in a simple ratio form. An unknown value can be calculated from the three known values of these imaging parameters. The image sensors are for the physical size of the imaging sensor which can be obtained, by industry and commercial standards format or size, when measured on their diagonal which is usually specified in $\frac{1}{1.7}, \frac{1}{2.5}, \frac{2}{3}, 1$ all in inches which can also be specified in mm in their product datasheets. Both the field of view and the focal length are dependent on the design and selection of the lens for the camera sensor. The main criteria being that the image sensor is overfilled with lens hence the diagonal size rather than the horizontal or vertical size usually published in their data sheets.The working distance is equivalent to the UAV altitude. The commercial sensors considered in this paper have specifications of expected ground resolution in cm/pixel at an assigned UAV altitude. For a given UAV equipped with a camera pay load, the resolution of the image will depend on the image sensor technology used e.g.megapixel HD etc. the number of photo-detectors inside these devices along the horizontal and vertical will determine the number of picture elements *pel* or along the horizontal and vertical array in the

image sensor itself by design that is h_{pel} and v_{pel} respectively. With the above development, we are now in the position to define what is called Ground Sampling Data or GSD to be:

$$GSD = \frac{s \times wd}{fl \times h_{pel}} \tag{10}$$

The above development shows that the Ground Sampling Data is therefore a function of the four most important UAV optical and flight variables that is $GSD = f\,(s, wd, fl, h_{pel})$. For typical values real device a dimension of 4896×3672 on its horizontal and vertical pixels, a focal length of 4.45 with a f-number of lens of 3.3 with an exposure time of 1/1,250, a horizontal field of view of 47.2 degrees are representative values for an image taken for a GSD=7cm/pixel at 180m altitude fpr example.

1.1.3 UAV sensor practical GSD performance

Here the horizontal fov is taken to be the image width along the horizontal that is h_{pel}. GSD will give unit measurements in [cm/pixel] or in units of [m/pixel] when all dimensions of length are converted to centimeters and meters respectively in the numerical calculation. An analysis of the datasheet for performance of two sensor class of a commercial UAV shows the GSD with lowering flight altitude in the following page. A representative performance of height to pixel resolution at ground of a commercial UAVfor RGB sensor only and for a Multispectral 5-band sensor (Airinov France) Model: eBee agricultural drone (Airinov Multispec 4mC Data Sheet.,2016) is shown below. As shown in Figure 2 and Figure 3 the published product datasheet pixel

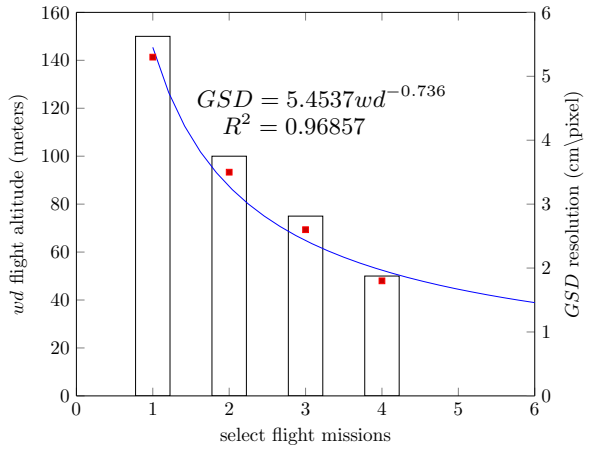

Figure 2: Reproduced from published datasheet of performance for an RGB only sensor shows an increasing resolution for lower flight altitudes at best with a GSD of 1.8cm/pixel@50m and of 5.2 cm/pixel@150m flight altitudes

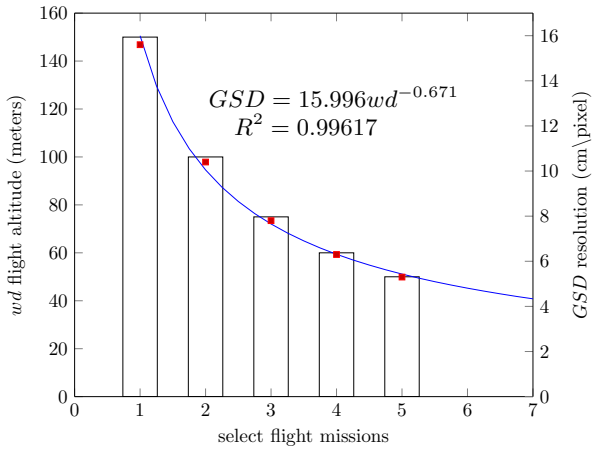

Figure 3: Reproduced from published datasheet of performance for a 5-Band Multispectral sensor shows an increasing resolution for lower flight altitudes at best with a GSD of 5.3 cm/pixel@50m and of 15.6 cm/pixel@150m flight altitudes

resolution increases with lowering flight altitudes. However, the increase is not linear possibly due to field of view and focal length of the lens varying with working distance or altitude inherent to the design of the lens itself. The lowest safe operating altitude of UAV is at 50m. However, suppliers can confirm that with change of safety features in software UAVs can operate at lower altitudes. Crops like corn, rice, wheat and vineyard crops are considered vegetations with low canopy heights which are less than 2 meters. On the other hand, safe flight mission is considered for vegetations like trees with canopy heights of 10m- 20m or higher. Hence the safe working distance of 50m is specified. We can see that for the RGB only sensor (Model Canon S110) and for the 5-band Multispectral sensor (Model Multispec m4C) power law curvefit when take that $y = GSD$ and $x = wd$ showing $R^2 \gg 95\%$ to be:

$$GSD_{rgb} = 5.4537wd^{-0.736} \tag{11}$$

$$GSD_{m4c} = 15.996wd^{-0.671} \tag{12}$$

The ebove equation can be used to compute for the greatest GSD at the lowest safe flight height. Assuming we are to survey and take images of low vegetation at a higher resolution with an assigned flight altitude of 20m, in theory, will result to $GSD_{rgb} = 0.6$cm/pixel and $GSD_{m4c} = 2.14$cm/pixel at ground.

2 DATA ACQUISITION AND SPECTRAL MEASUREMENT SET UP

We set-up a basic workflow shown in Figure 4 below. It that starts from the data acquisition from flight missions at two different altitudes, a low and high altitude. The devices are composed of two different sensors - a high resolution RGB bands only (Canon S110) and a Red Edge multispectral 5-band sensor having RGB+RE+NIR. The flight happens in sequence for a selected predetermined test station in a 27,000 hectare of pineapple farm field. The raster images are preprocessed, conditioned and orthocorrected, mosaicked in using UAV software (Pix4D). The vegetation indices NDVI, GRVI,GR, EVI, CIgreen, CIred (Via, A. et al.,2011) are obtained by performing band mathematics using open QGIS, MultiSpec and GRASS GIS. The NDVI having two values to compare coming from the UAV software and those from results of band mathematics. It is followed by a local

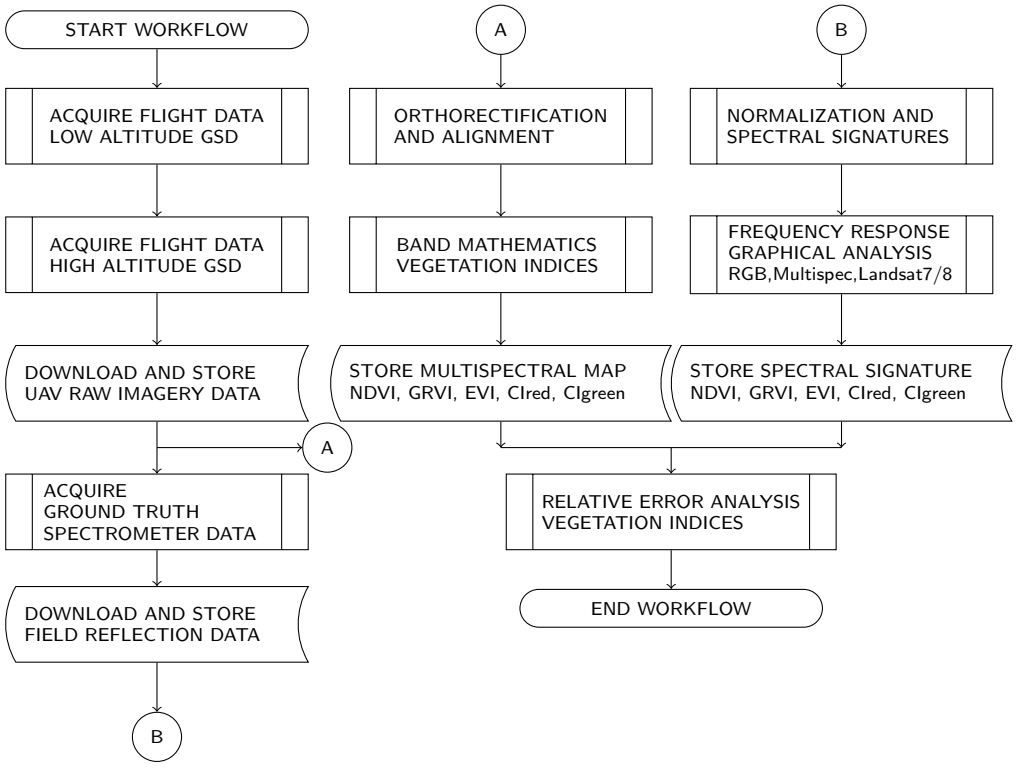

Figure 4: Basic workflow for the study for evaluating the spectral response performance of two selected commercial sensors from resolution to calculation of vegetation indices

field validation from selected test station which the flights has covered A second set of data concerns itself with the gathering of spectral data. We obtain the raw spectral data using a hand held spectrometer (Ocean Optics USB 650). To arrive at the spectral signature we perform a post processing to obtain normalized spectra. The plot of spectral signatures will be then used for a frequency and graphical analysis with the bands of the sensors a to arrive a the values of NDVI, GRVI, EVI, CIgree, CIred vegetation indices. this short study only considered healthy plant and those having matured canopy area (Nagai S.,2012).

3 DATA PROCESSING RESULTS AND DISCUSSION

The sample flight data were obtained from a fixed wing UAV Model: eBee (Airinov France) they are representative only of the large amount of imagery available. For the purposes of this paper we use them to illustrate the actual performance as discussed in the previous sections. The spectral response curves for the sensors were obtained from product datasheet and available graphic at the manufacturers website, user manuals and documentation from the providers Airinov's 4mC and Micasense's Rededge they were largely obtained from their product website. The Landsat 8 OLI bands are from the USGS website. Images are specified to be at their GSD of [cm/pixel] at flight altitude in meters. The data set were post processed using open source and freely available software QGIS Ver.2.14.1, MultiSpec Ver.3.5 (University of Purdue), GRASS GIS Ver.7.0 and image processing tool ImageJ (NIH US).

3.1 Visible bands imagery acquisition results from UAV flights

Shown in Figure 5 are representative imagery for a high resolution 3-band RGB only sensor taken at a low and high altitude setting. We select GRVI for the RGB only sensor and NDVI for the multispectral sensor for viewing the results of the band mathematics operation based on formula in Table 1. The GRVI shows clearly the indication of the presence of high vegetation e.g.trees, bamboos at the periphery of the plantation as well as roads and canals, the yellowing areas clearly delineates the class for the plants specially at higher altitudes.

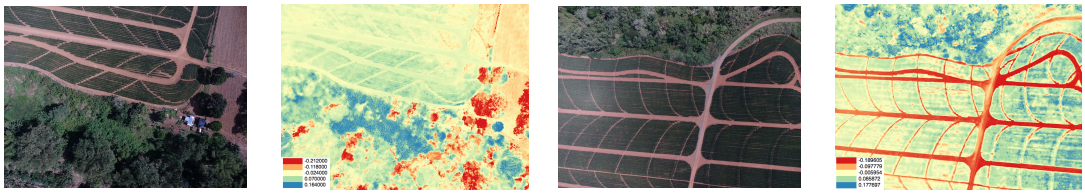

(a) RGB from S110 1.8cm/pixel@50m

(b) GRVI from RGB of S110 1.8cm/pixel@50m

(c) RGB from S110 7cm/pixel@180m

(d) GRVI for RGB from S110 7cm/pixel@180m

Figure 5: Sample images from composite of RGB taken with Airinov UAV Canon S110 camera with an image 4896×3672 pixels resolution, lens focal length of 4.45 representative of a low and high flight altitude

3.2 Multispectral bands imagery acquisition results from UAV flights

We show the sample imagery in Figure 6 below, one with a low 50m and a 150m altitude bringing two different GSD resolution from the output of a 4-band multispectral sensor. The image sample was produced from the discrete and non-overlapping bands of the channels G,R,RE and NIR. The Airinov Model 4mC is a 4-band mutispectral camera with out a Blue channel. Stacking the color planes brings vegetation and soil clearly differentiated. NDVI was chosen to be the metric for these samples. As we observed there is considerable influence of high vegetation in the numerical result at the height from data acquisition.

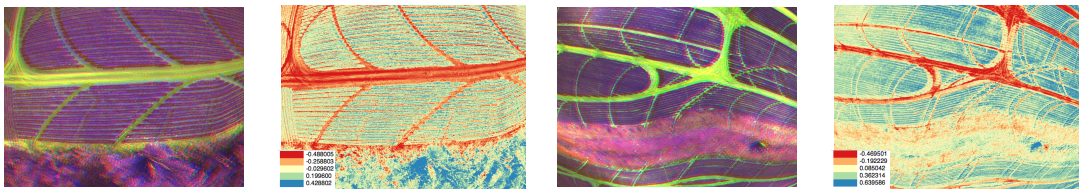

(a) 4-band stacking from 4mC imagery at 5.3cm/pixel@50m

(b) GRVI from 4mC Green-Red band at 5.3wcm/pixel@50m

(c) 4-band stacking from 4mC imagery at 15.7cm/pixel@150m

(d) NDVI from 4mC Red-NIR band at 15.7cm/pixel@150m

Figure 6: Sample images for multispectral composite with 1280×960 pixels resolution from Airinov UAV multispectral sensor Model m4C with lens of focal length at 3.6 representative for a low and high flight altitude

3.3 Band Math results for visualization of selected vegetation indices

This paper focuses on a set of preselected vegetation indices that mainly uses the visible bands (RGB) and the near infrared band (NIR). We reference to the article published (Via, A. 2011) where we obtain the following formulas to implement the band mathematics (Nagai,S. 2012) shown in Table 1

Table 1: Selected Vegetation Indices

Definition	Formula	Reference
Green Ratio Vegetation Index	$GR = \frac{NIR}{Green}$	Sripada, R., et al(2006)
Simple Ratio	$RVI = \frac{NIR}{Red}$	Jordan(1969)
Green Red Vegetation Index	$GRVI = \frac{Green-Red}{Red+Green}$	Rouse et al.,(1974)
Normalized Difference Vegetation Index	$NDVI = \frac{NIR-Red}{Red+NIR}$	Rouse et al.,1974)
Ehnanced Vegetation Index	$EVI = 2.5\left(\frac{NIR-Red}{NIR+6Red-7.5Blue+1}\right)$	Huete et al.,(1996),(1997)
Green Chlorophyll Index	$CI_{green} = \frac{NIR}{Green} - 1$	Gitelson et al.,(2003a,c),(2005)
Red Edge Chlorophyll Index	$CI_{rededge} = \frac{NIR}{RedEdge} - 1$	Gitelson et al.,(2003a,c),(2005)

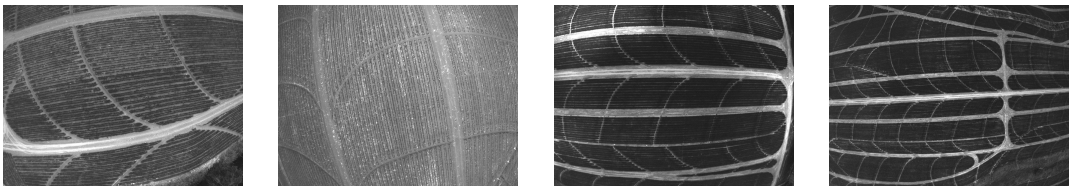

(a) Green from 4mC 5.3cm/pixel@50m

(b) Green from 4mC 7.8cm/pixel@75m

(c) Green from 4mC 15.7cm/pixel@150m

(d) Green from 4mC 23.5cm/pixel@225m

(e) RGB from S110 1.8cm/pixel@50m

(f) RGB from S110 15.7cmp/pixel@150m

(g) RGB from S110 5cm@175m

(h) RGB from S110 7.4cm/pixel@250m

Figure 7: Representative multispectral images acquired from Airinov 4mC Multispectral sensor and RGB imagery acquired from Canon S110 RGB sensor

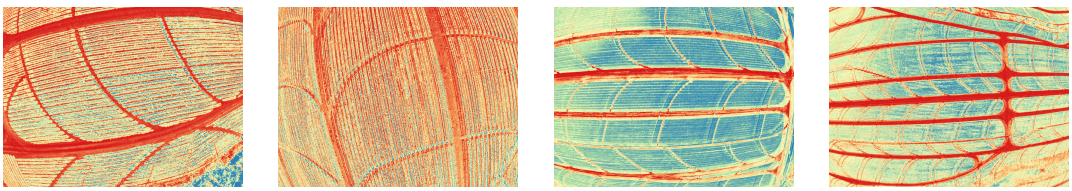

(a) GR from 4mC 5.3cm/pixel@50m

(b) RVI from 4mC 7.8cm/pixel@75m

(c) NDVI from 4mC 15.7cm/pixel@150m

(d) CIgreen from 4mC 23.5cm/pixel@225m

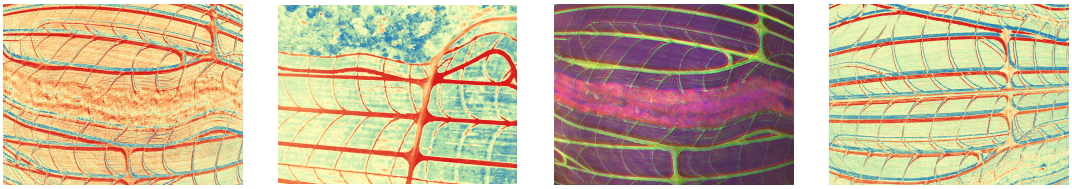

(e) CIrededge from 4mC 23.5cm/pixel@225m

(f) GRVI from S110 7cm/pixel@180m

(g) 4-band composite from 4mC imagery

(h) NDVI Red Edge 23cm/pixel@225m

Figure 8: Representative raster images from Band Mathematics operation using imagery from Airinov 4mC Multispectral sensor and Canon S110 RGB sensor

3.4 Ground truth spectral signature acquisition of specimen plant

For purposes of establishing some baseline data, specimen plant were preselected from various test stations.The criteria is for a healthy and mature at their stage however, they are not are not either bearing fruit or at harvesting stage but simply those having a full blown canopy.The field data was obtained on site using a handheld spectrometer (USB 650 Ocean Optics US) and data was preprocessed by spreadsheet macro file.

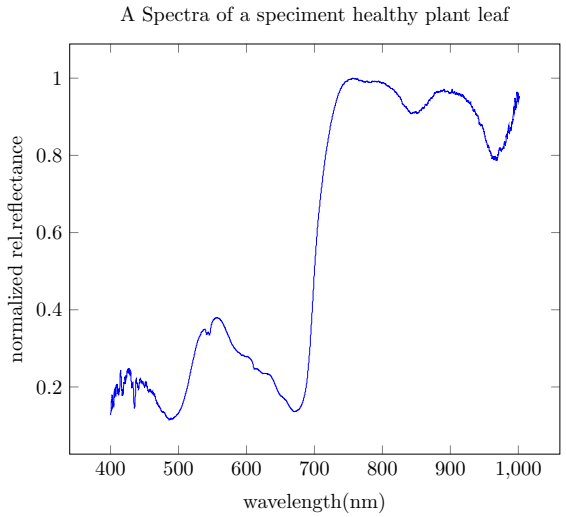

Figure 9: The spectra of a leaf taken from a specimen plant is shown from 400nm-1000nm

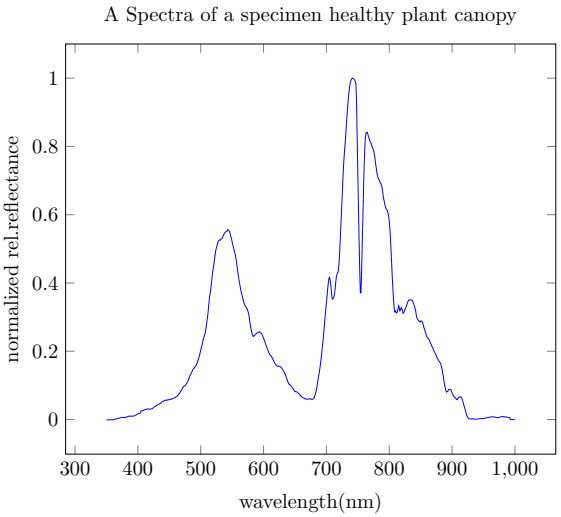

Figure 10: The spectra of a plant canopy from a specimen plant is shown from 400nm-1000nm

3.5 Frequency analysis results from spectral response UAV sensors and Landsat 8 OLI with Spectral Signature

In Figure 11 we show the spectral sensitivity plot for the 4-band Airinov Model 4mC sensor as well with Figure 12 for the Micasense Red Edge spectral response for the 5-band sensor. A key differentiation between them is the absence of the Blue band in Model m4C however, there is larger gain in it's NIR and in the Red band. We also see that the location of their central frequencies and their spectral widths are also different from each sensor. We select those vegetation indices as they are able to be calculated from the sensor's available bands as shown inside these multi-plots. Following the same method from Landsat (USGSa.,2016) The peak response are obtained under the response curve as marked.

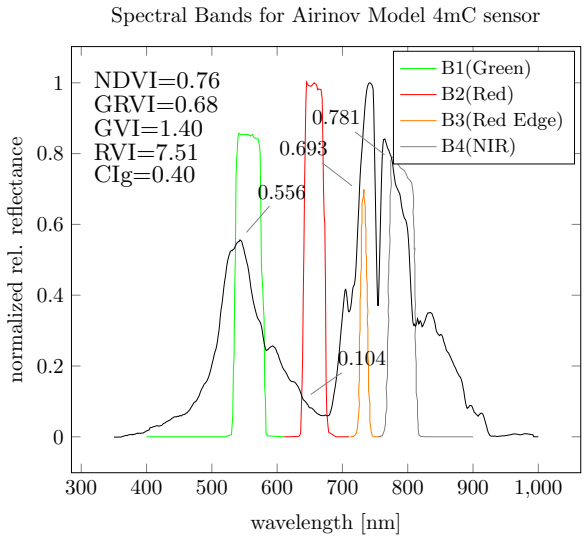

Figure 11: The discrete 4-band spectral response of the Airinov Model:4mC camera sensor gives Green, Red, Red Edge and NIR band without the Blue band

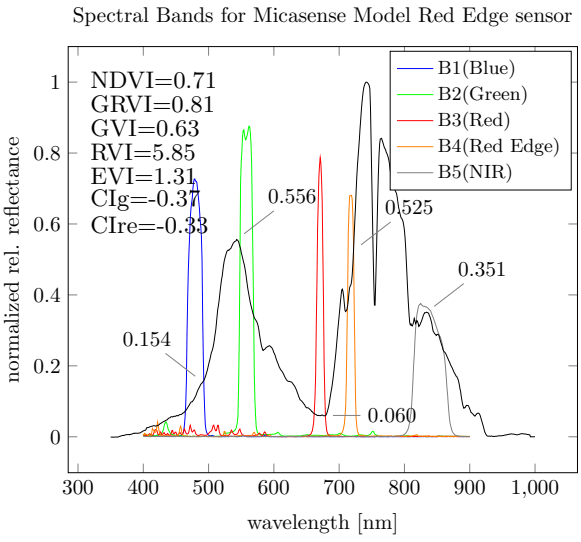

Figure 12: The discrete 5-band spectral response of the Micansense Model:Red Edge camera sensor gives Blue, Green,Red, Red Edge and NIR bands

Prior to UAV technology based photogrammetry, flights for multispectral class data acquisition for agricultural assessment, satellite imagery was the only available means to obtain them, it is the interest of the authors to compare the Landsat 8 OL in their relative spectral response with the modern UAV this we shown in Figure 13 for the entire band and in Figure 14 for the visible wavelengths bands.We can distinguish the very high sensitivity of the the Landsat 8 OLI sensors and their spacing in frequency as compared with UAV sensors.However, there is no Red Edge band present in Landsat8 bands they however can extend beyond the 1000nm limiting case for the UAV sensors. Overlaying the spectral signature of the plant to obtain the simulated sensor response.

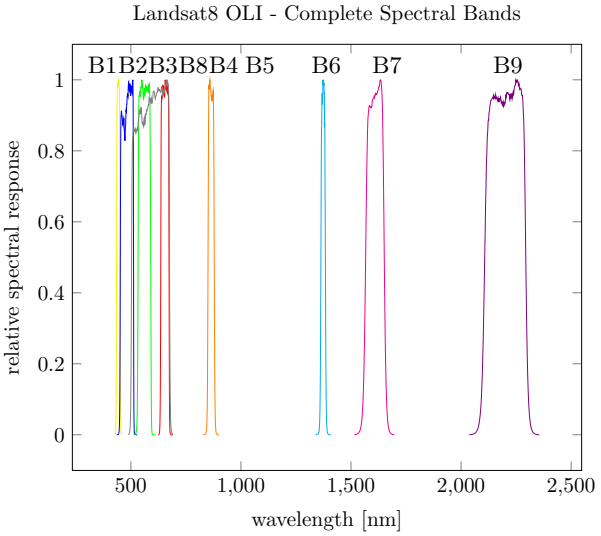

Figure 13: The Landsat 8 is a 30m resolution satellite composed 5 visible bands and 4 invisible bands with a 15m panchromatic band (Band 8) that could be used to increase the resolution in the visible bands by numerical integration.

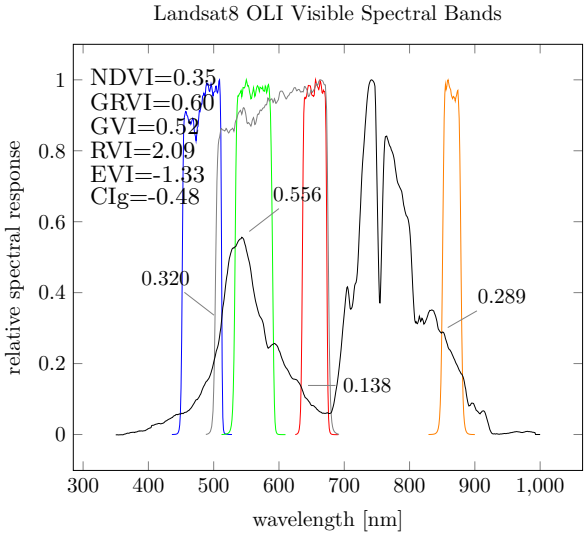

Figure 14: The Landsat 8 visible bands relevant to the calculation of vegetation indices are shown. The spectral signature of the specimen plant is overlaid and spans all the bands B-G-R, NIR (30m) and the Panchromatic band (15m).

3.6 Error Analysis between sensor bands from vegetation indices results

We now compare the relative difference of results from graphical analysis results from the spectral response of the sensors from Aironov multispectral sensor 4mC and Micansense Red Edge sensor and the USGS Landsat 8 OLI with the field measured spectral signature of the plant obtained from field spectrometer. We define the relative error in Equation 13 and the and the percentage difference when comparing between sensors we define in Equation 14. It is to be noted that ground truth band vegetation indices were from the result of graphical frequency analysis while the sensor band were obtained from results of band mathematics using QGIS raster calculator. Error analysis results are shown in Table 2 and Table 3 below:

$$\%\ rel.err = \frac{|Ground\ Truth\ Band - Sensor\ Band\ Data|}{Ground\ Truth\ Band} \times 100\% \tag{13}$$

$$\%\ p.err = \frac{|Sensor\ Band\ Data_1 - Sensor\ Band\ Data_2|}{Sensor\ Band\ Data_1} \times 100\% \tag{14}$$

Table 2: Relative Error Ground Truth Band to Sensor Bands

Vegetation Index	Spectral Sig. → 4mC	Spectral Sig. → RE	Spectral Sig. → Landsat 8
GRVI	37%	47%	29%
NDVI	16%	18%	21%

Table 3: Percentage Error Sensor to Sensor difference

Vegetation Index	4mC → RE	RE→ 4mC	4mC. → Landsat 8	RE → Landsat8
GRVI	18%	15%	12%	25%
NDVI	7%	8%	54%	50%

4 CONCLUSIONS AND RECOMMENDATIONS

We have shown in the development of this paper that the geometry involving the optical, flight height and horizontal field of view are truly the interacting key parameters to consider in operating the UAV. The spectral response of the sensors their center frequency location, bandwidth and their sensitivity will ultimately determine their measurement of vegetation indices as they will provide the gain under the bands. By determining the spectral signature of plant specimen of their leaf and canopy spectra will provide knowledge of the dynamics where they will lie in a sensor. The Red-NIR band will have to be engineered or tailor fit based the plant reflectance dynamics. The numerical results using simulated frequency response plots points the Airinov m4C sensor is superior in these bands however the absence of a Blue band brings about considering a pure RGB sensor Canon S110 for visualization in GR, GRVI. Micasense bring all the bands together in one sensor however is short the sensitivity in the NIR however the pixel resolution is superior for a whole 5-band sensor in one single package. A larger data set composed of several tiles of raster of images maybe needed in the immediate future for further validating these results.

Acknowledgments

We would like to thank firstly the PCIEERD from the national Department of Science and Technology (DOST) for their support for the Philippine LiDAR Resource Mapping project specially the provision for the funds for the field spectrometer. To our generous corporate co-authors and company the Del Monte Company Philippines Inc. from the pineapple plantation in Manolo Fortich in Bukidnon, Cagayan de Oro province for sponsoring the first author in several plantation visits and flight missions. We thank the Department of Geomatics and Analytics with their senior manager Mr. Benjamin Manbanta with his lead and innovations for leading the UAV team and specially providing the authors with sample clips test data sets from actual flight mission enabling us to evaluate by way of simulated response of the sensors. The project leader and co-author Dr. Roland Otadoy, the Chiefs, Engr.Aure Oraya of LiDAR1 and Renante Violanda of LIDAR2 components for the time and resources in the development of this paper at the USC Phil-LiDAR Research Center. Dr. Danilo Dy and Prof. Annie Diola from the Department of Biology for the discussion on plant biology. Equally with great thanks to Mrs. Revian Mangubat Manhuyod an english major and educator for her proofreading and providing corrections to this manuscript.

References

Airinov Multispec 4mC Data Sheet., Retrieved August 31, 2016, from
http://www.airinov.fr/en/uav-sensor/agrosensor/

Business Insider The Drones Report: Market forecasts, regulatory barriers, top vendors, and leading commercial applications., Retrieved August 31, 2016, from
http://www.businessinsider.com/uav-or-commercial-drone-market-forecast-2015-2

Gitelson, A., 2004. Wide Dynamic Range Vegetation Index for Remote Quantification of Biophysical Characteristics of Vegetation. Journal of Plant Physiology, 161(2), pp.165-173

Hiroyuki, M. et al., 2012. Spectral vegetation indices as the indicator of canopy photosynthetic productivity in a deciduous broadleaf forest. Journal of Plant Ecology, 6(5), pp.393-407

USGS.,2016a. Landsat Bands Spectral viewer., Retrieved August 31, 2016, from
http://landsat.usgs.gov/tools_spectralViewer.php

USGS.,2016b. Landsat 8 Spectral Response of the Operational Land Imager In-Band, Band-Average Relative Spectral Response Retrieved August 31, 2016, from
http://landsat.gsfc.nasa.gov/?p=5779

Micasense Red Edge Data Sheet., Retrieved August 31, 2016, from
http://www.micasense.com/rededge/

Nagai, S. et al., 2012. In situ examination of the relationship between various vegetation indices and canopy phenology in an evergreen coniferous forest, Japan. International Journal of Remote Sensing,
33(19) pp.6202-6214

Via, A. et al., , 2011. Comparison of different vegetation indices for the remote assessment of green leaf area index of crops. Remote Sensing of Environment,115(12), pp.3468-3478